

# Effect of Coal-Rock Interface Properties on Failure Stability of Coal Pillars Expressed in Energy Terms

Zhang, K.

Poeck, E. Garvey, R. and Ozbay, U.

*Colorado School of Mines, Golden, Colorado, USA*

Copyright 2015 ARMA, American Rock Mechanics Association

This paper was prepared for presentation at the 49<sup>th</sup> US Rock Mechanics / Geomechanics Symposium held in San Francisco, CA, USA, 28 June-1 July 2015.

This paper was selected for presentation at the symposium by an ARMA Technical Program Committee based on a technical and critical review of the paper by a minimum of two technical reviewers. The material, as presented, does not necessarily reflect any position of ARMA, its officers, or members. Electronic reproduction, distribution, or storage of any part of this paper for commercial purposes without the written consent of ARMA is prohibited. Permission to reproduce in print is restricted to an abstract of not more than 200 words; illustrations may not be copied. The abstract must contain conspicuous acknowledgement of where and by whom the paper was presented.

**ABSTRACT:** Rockbursts, or coal bumps in coal mines, involve the spontaneous, violent fracture of rock. This paper discusses the application of energy concepts to back-analysis studies of coal bump events. Two-dimensional distinct element models were constructed of coal pillars with a range of material properties assigned to both coal material and rock-coal interfaces. These models were used to explore the compounding effects of the brittle failures of coal material and coal-rock interfaces on the energy release magnitudes. Loading conditions applied to these models represent a pillar failing individually as well as a full panel collapse. Results from the pillar models are presented in terms of the kinetic energy released from the unstable failures. Due to variation of coal and coal-rock interface properties, the magnitude of the excess kinetic energy was found to vary significantly. The total magnitude of kinetic energy released from the models was found to be significantly higher when brittle failure behavior was assigned to both the coal and to the coal-rock interface. This increase in excess energy indicated larger unstable failures and higher dynamic efficiencies under such material combination. In addition to the methodology for analyzing the effect of coal material and interface properties on the pillar failure stability, the paper also introduces and demonstrates a feasible failure mode for large width-height ratio pillars.

## 1. INTRODUCTION

Compressive and shear slip failures emerge in deep underground mines under the influence of mining activities. Historically, several research efforts were made to address the role of excess energy on the initiation and occurrence of rockbursts, which included the Energy Release Rate (ERR) concept proposed by Cook [1] and Excess Shear Stress (ESS) presented by Ryder [2]. However, neither of these approaches accounts for brittle failure of rock and they have therefore not been ordinarily applied to study rockburst or coal bump incidents. In this paper, the commercially available software Universal Distinct Element Code (UDEC) is used to numerically model the failure instabilities and to present an illustration based on the unstable excess energy concept.

UDEC maintains the ability to simulate the quasi-brittle behavior of discontinuities through the Continuous-yielding (CY) joint property [3, 4]. The Mohr-Coulomb strain-softening (MCSS) constitutive model may then be

used to represent quasi-brittle material failure during unstable loading conditions [5]. The program also calculates the kinetic energy released and ultimately damped out during the simulation. A series of single pillar models were built with these combinations of tools to better understand the mechanism of bumps within wide coal pillars.

## 2. METHODOLOGY

The stability of compressive failures was described by Cook [6] through the analogy to the stiffness of a UCS testing machine under compressive stresses. If the energy released by the system surrounding the rock is in excess to that which can be consumed during failure, then unstable failure occurs in the rock. Besides direct compression, there is another mechanism for the unstable failure to occur which is through the sudden removal of confining pressures from highly stressed rock. With a high vertical stress applied onto the system, unstable slip failures which occur along coal-rock interfaces may trigger sudden de-confinement to the

mining faces or sidewalls, leading to powerful unstable failures.

Several researchers have studied the effect of shear failure on the loss of pillar strength [7, 8]. However, these studies were not extended to exploring the effect of sudden slip failure. In this paper, the effect of the coal-rock interface is demonstrated through the release of kinetic energy to quantify the magnitude of unstable failure.

When the load is applied to the block system shown in Fig. 1, all energy within the system can be accounted for in the quasi-static energy balance equation given as

$$W_b = U_c + W_p$$

In this scenario, the block is assumed to deform in a stable manner. Boundary work,  $W_b$ , is first added through the constant pressure  $P$  applied on top. This boundary work is then stored as strain energy in the rock mass as  $U_c$ . When failure initiates under increased  $P$ , a plastic work,  $W_p$ , is performed within the system.

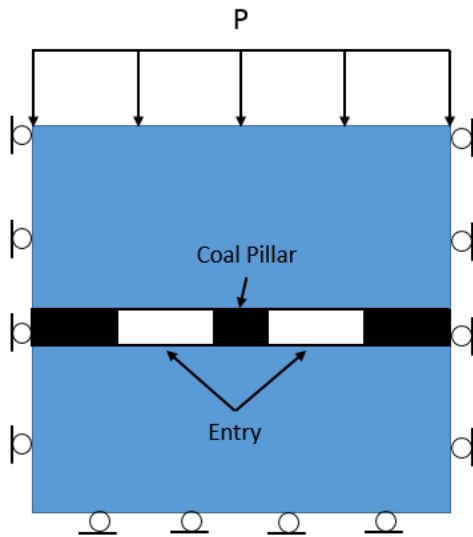


Fig. 1. Rock mass loaded with boundary work

If unstable failure also occurs in the system, an additional term for kinetic energy needs to be included to account for the energy released during failure. In UDEC, the excess energy magnitudes resulting from the unstable failures can be determined using static or dynamic calculations [4]. For the static approach, the excess energy is calculated as the difference between the energy applied to the system and the energy which is stored and consumed within the system. Unstable excess energy  $E_u$ , which is equivalent to the kinetic energy released due to dynamic instability in the system, can be expressed as

$$E_u = W_b - (U_c + W_p)$$

The dynamic excess energy calculation can be made based on the current kinetic energy,  $E_k$ , and total damped work,  $W_d$ , as shown in the equation below:

$$E_u = E_k + W_d$$

Theoretically, the two methods of calculating  $E_u$ , should be identical, whose magnitude is equal to the kinetic energy released due to unstable failure provided any external loading is applied in a quasi-static manner. In the single pillar models that are studied in this paper, the difference between the static calculation and dynamic calculation accounts to less than 0.4%. In this paper, the dynamic calculation of unstable excess energy is taken for further study.

### 3. SINGLE PILLAR MODEL FOR THE BACK-ANALYSIS OF CRANDALL CANYON MINE COLLAPSE

#### 3.1. Single Pillar Model Geometry and Boundary Conditions

The following series of single pillar models were built as analogues to the pillar failure observed in the Crandall Canyon collapse of 2007 [9]. Three pillar types from this collapse case were considered, namely north barrier pillar, south barrier pillar, and south barrier pillar in retreat. All models assume a half-symmetry condition by applying horizontal constraint along the sides of the model. Fig. 2 shows the geometries of the single pillar models, where a 0.4m zone size was used to represent coal material within a 4m thick seam. The pillar height was taken as 2.4m for models of pillars from the north barrier and south barrier sections in the Crandall Canyon mine prior to collapse. A coal pillar height of 4m was assumed in the South barrier to represent pillar geometries which were developed during retreat mining. The model maintained a total height of 34.4m and an entry width of 3.2m in all cases.

For the north barrier (Fig. 2A), the pillar half-width was taken as 9.0m for a width-to-height ratio of 7.5. The south barrier pillar had a slightly wider half-width of 9.4m and was modeled with and without floor coal mining as shown in Fig. 2B and 2C.

The bottom of the model was fixed in the vertical direction and external loading was applied from the top of the model until a target strain of 0.025 was reached.

#### 3.2. Pillar loading

Fig. 3 shows different loading curves to illustrate quasi-brittle material behavior and different loading conditions which were applied onto the pillar and throughout

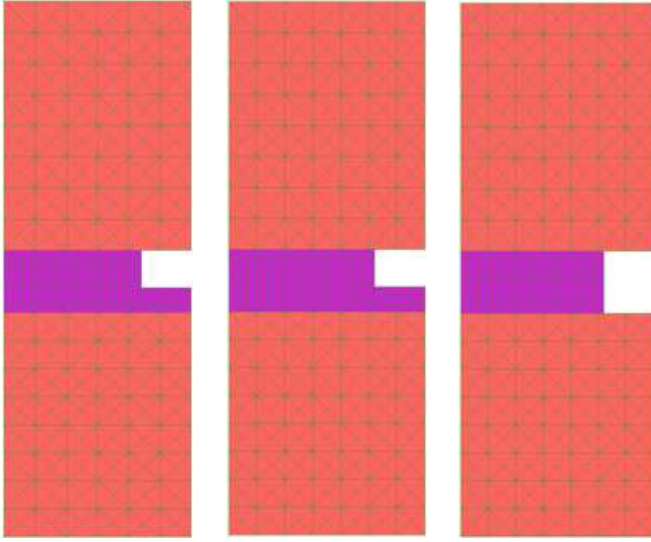


Fig. 2. Single pillar models: North Barrier (left), South Barrier (middle), and South Barrier Pillar in Retreat (right).

its ultimate failure. A pressure-based loading was applied to pillars to simulate a constant overburden loading that assumes zero stiffness,  $k_p$ . A displacement-based loading condition was used to represent individual pillars failing due to elastic rebound of the surrounding rock mass whose loading stiffness is represented by  $k_d$ . The area between a load line and the pillar response is the energy released as excess kinetic energy per unit area of coal. If the loading stiffness is the only variant in a model, then the excess energy released from the model with pressure boundary loading must be higher than that of the displacement loading condition.

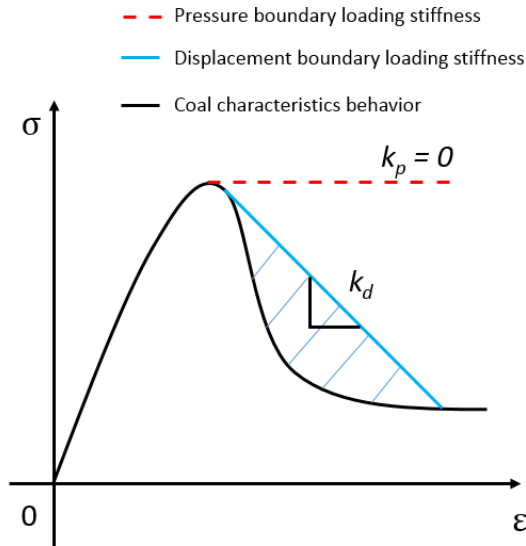


Fig. 3. The stiffness of loading system with different loading conditions as implemented in UDEC.

### 3.3. Model material properties

Elastic, Coulomb slip (CS), and CY joint constitutive models were used to represent the interfaces between the

coal and the surrounding rock. The coal was given elastic, Mohr-Coulomb (MC) or MCSS material properties.

The parameters of the coal-rock interface property used for the single pillar models are listed in Tables 1 and 2, which are for the MC and CY joint interfaces models. The parameters of rock mass mechanical properties used for the MCSS coal material are listed in Table 3. These initial data of rock mass mechanical property were extensively calibrated by Gu [10]. We only consider Class-I type post failure behavior of coal in this case.

Table 1. Calibrated input parameters used for the CS joint model.

Description	Value	
Joint normal stiffness	50	GPa/m
Joint shear stiffness	50	GPa/m
Joint cohesion	0	GPa
Joint friction angle	20	deg
Joint dilation angle	0	deg
Joint tensile strength	0	GPa

Table 2. Calibrated input parameters used for the CY joint model.

Description	Value	
Joint normal stiffness	50	GPa/m
Joint shear stiffness	50	GPa/m
Joint normal stiffness exponent	0	-
Joint shear stiffness exponent	0	-
Joint intrinsic friction angle	15	deg
Joint initial friction angle	40	deg
Joint roughness parameter	0.15	Mm

Table 3. Calibrated input parameter tables used for MCSS coal material.

Cohesion plastic strain, cohesion (MPa)	0	1.69
	8e-5	1.47
	0.035	0.2
Friction Angle plastic strain, friction angle (deg)	0	23
	7e-5	27.5
	1e-4	30
Dilation Angle (plastic strain, dilation/deg.)	0	2
	7.2e-5	10
	1	2

## 4. RESULTS AND DISCUSSIONS

### 4.1. Displacement loading

The result from the model of south barrier pillar with CY joint and MCSS coal property helps demonstrate the relationship between excess energy trends and the occurrence of unstable pillar failure. The loading condition is displacement based in this scenario. For the analysis, the pillar is divided into eight sections, shown in Fig. 4 for the analyses of localized stress.

As shown in Fig. 5a, average stress vs. numerical time behavior of the south barrier pillar model exhibits plastic failure and there is no significant stress drop for the average stress during the loading process, which would indicate a whole pillar failure. Some smaller, localized instabilities emerged within portions of the pillar rib without affecting the overall strength of the pillar. These localized unstable failures are difficult to discern purely from stress behavior, but become apparent from the released kinetic energy, which can be demonstrated from Fig. 5b. It can be seen that several obvious damped work increase as the loading applied onto the system.

Fig. 6a demonstrates that the coal in Section 8 reached its peak strength, and experienced a sudden stress drop due to unstable failure conditions in the pillar rib. Then Fig. 6b shows that Section 7 of the pillar failed due to the de-confinement by Section 8, leading to another damped work increase. Afterwards, with continuing loads applied to the model, Section 6 of the pillar failed unstably, as shown in Fig. 6c, which accounted for the increasing amount of the damped work.

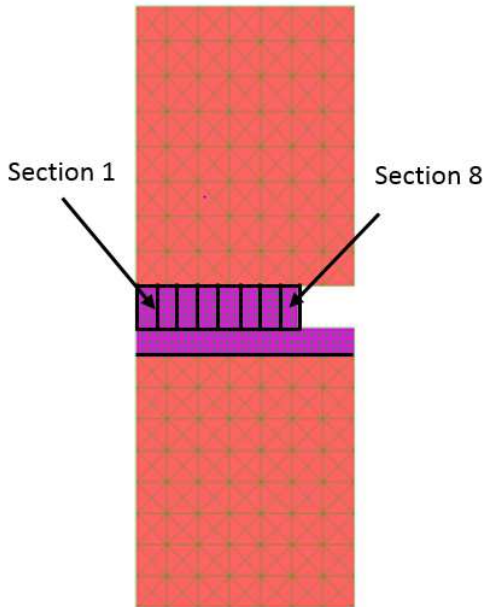
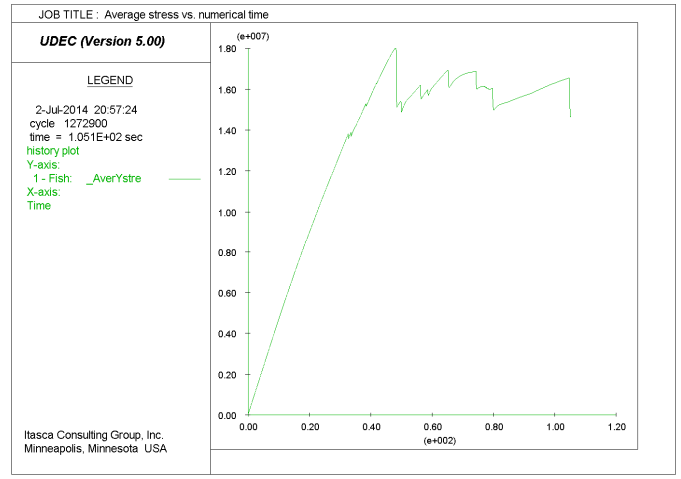
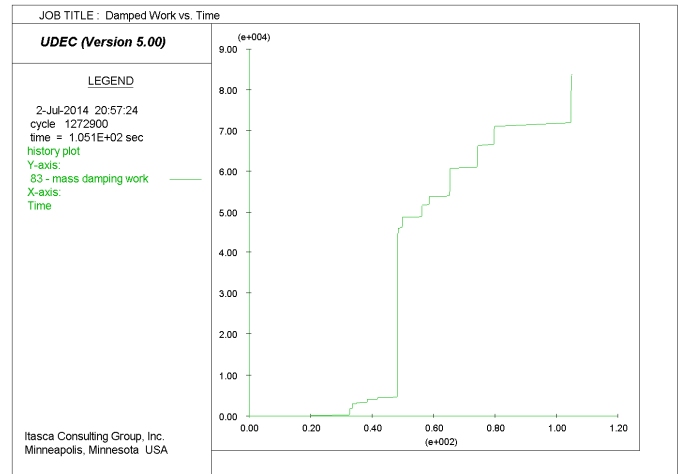


Fig. 4. Single pillar model (slices view)



(a)



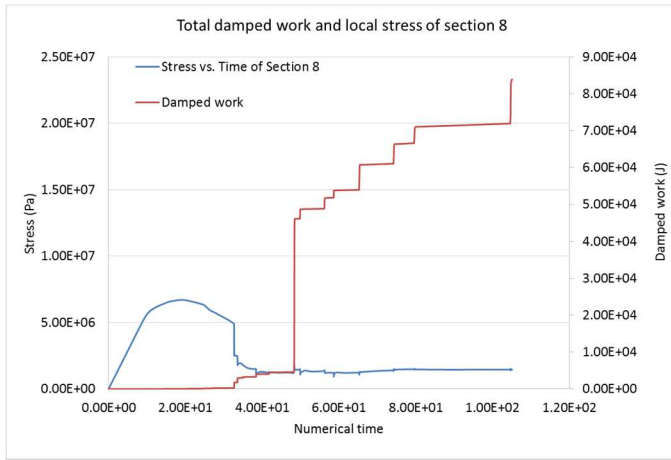
(b)

Fig. 5.( a) Average stress vs. numerical time for south barrier pillar model under displacement loading and (b) damped work vs numerical time

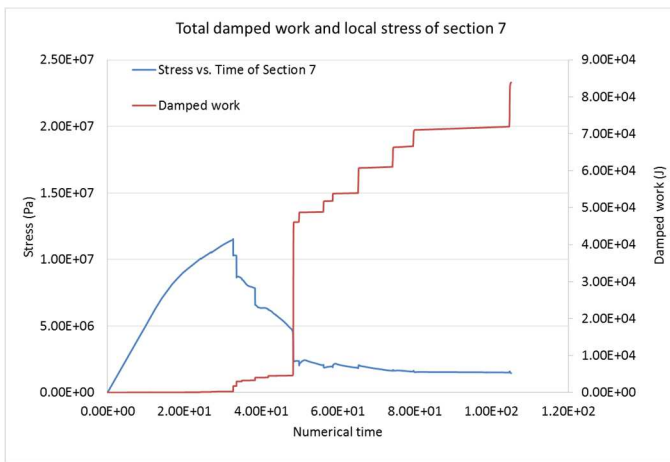
When Section 6 of the pillar failed, the damped work increased about 41,000 J, resulting from a release of excess energy. Even though the overall stress vs time behavior made the pillar failure appear plastic in nature as in Fig. 5a, the pillar rib of Section 6 still failed in an unstable manner. The energy shown by red plot line in Fig. 6, demonstrates a corresponding increase of damped work during this same period of instability.

### 4.2. Boundary pressure loading conditions

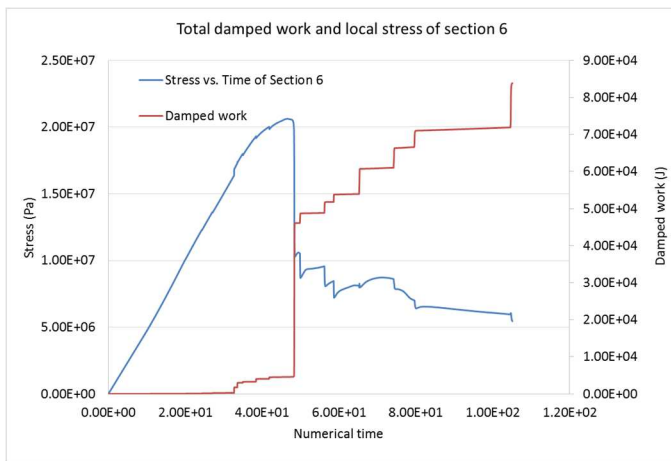
The results of the MCSS-CY models loaded under pressure loading conditions applied to the top boundary are reported in Table 4. The combination of a brittle constitutive law applied to both the coal and coal-rock interface was found to release the largest magnitudes of excess energy when expressed in proportion to the energy supplied to the system through external boundary work. These results are provided in terms of total released energy to total energy supplied to the system. They show that the percentage of unstable excess energy to total boundary work reaches 5.30% for the 2D quasi-brittle pillar models.



(a)



(b)



(c)

Fig. 6. Damped work and stress conditions of (a) Section 8 vs numerical time, (b) Section 7 vs. numerical time, and (c) Section 6 vs numerical time.

The excess energy values from each pillar test are summarized in Fig. 7. As seen, the models with a pressure loading condition give a much higher excess

Table 4. The percentage of excess energy over boundary loading work ( $E_u/W_b$ )

Pillar Geometry	Loading Conditions	$E_u/W_b$
North barrier	Pressure	3.20%
	Displacement	0.10%
South barrier	Pressure	2.70%
	Displacement	0.65%
South barrier in retreat	Pressure	5.30%
	Displacement	0.93%

energy value than the models where displacement loading is applied. This fact can be explained by the difference in stiffness between pressure and displacement based loading systems given in Fig. 3.

## 5. CONCLUSIONS

The single pillar modeling studies demonstrate the emergence of unstable failure conditions through the excess energy results. In line with the theoretical thinking of Cook [6] and Rice [11], the potential coal bump events can be numerically simulated in a quantitative way based on the energy calculation method of excess energy during failure.

Generally, there is a significant increase in excess energy when the CY model is used compared to the CS joint model. Also, the excess energy has a great boost when the MCSS model is applied as opposed to the MC coal material. The largest excess energy release was associated with the case of using the MCSS model as the coal material and CY joint as the coal/rock interface in the case of south barrier retreat.

The results also show that the energy calculation method introduced in this paper can assist in analyzing the mechanism of coal bumps. Further research through extensive backanalysis studies can lead to even more accurate understanding of how coal bumps as they occur in full mine models, which in turn may provide a more comprehensive understanding of coal bump events.

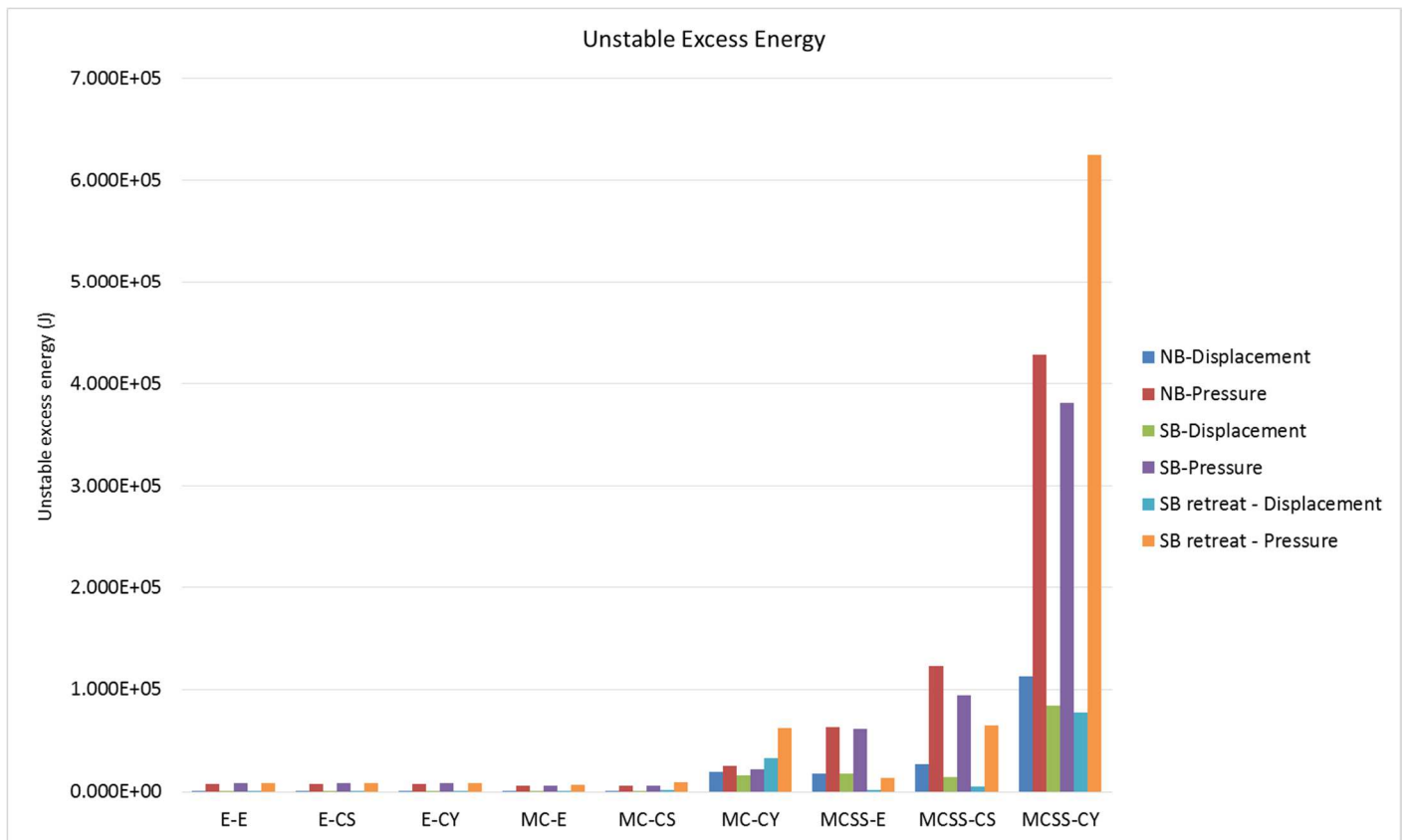


Fig. 7. Excess energy values for different single pillar with different coal-rock properties. On the horizontal axis, letters before and after the dash line refers to coal material and interface constitutive model type, respectively.

## 6. ACKNOWLEDGEMENTS

The work presented in this publication is part of an ongoing research activity conducted at the Colorado School of Mines which has been generously funded by the ALPHA Foundation. The contents of this publication are solely the responsibility of the authors and do not necessarily represent the official views of ALPHA Foundation.

## 7. REFERENCES

- Cook, N. G. W. 1966. The design of underground excavations. In *The 8th US Symposium on Rock Mechanics (USRMS)*. American Rock Mechanics Association. 1967;167-193
- Ryder, J. A. 1988. Excess shear stress in the assessment of geologically hazardous situations. *Journal of the South African institute of Mining and Metallurgy*, 88(1), 27-39.
- Gu, R., & Ozbay, U. 2012. Distinct element model analysis of unstable failure of rock discontinuities. In: *Proceedings of the 46th US Rock Mechanics/Geomechanics Symposium*, Chicago, IL, USA; 24-27 June 2012.
- Itasca Consulting Group, 2010. UDEC (Universal Distinct Element Code), Version 5.0. Minneapolis, MN.
- Kias, E. M. C., Gu, R., Garvey, R., & Ozbay, U. 2011. Modeling unstable rock failure during a uniaxial compressive strength test. In *Proceedings of 45th US Rock Mechanics/Geomechanics Symposium*, San Francisco, CA, 26-29 June 2011 (pp. 825-833).
- Cook, N. G. W. 1965. A note on rockbursts considered as a problem of stability. *JS Afr. Inst. Min. Metall.*, 65(3), 437-446.
- Esterhuizen, E., Mark, C., & Murphy, M. M. 2010. Numerical model calibration for simulating coal pillars, gob and overburden response. In *Proceeding of the 29th international conference on ground control in mining*, Morgantown, WV (pp. 46-57).
- Iannacchione, A. T. 1990. The effects of roof and floor interface slip on coal pillar behavior. In *Proceedings of the 31st US Symposium on Rock Mechanics* (pp. 156-160).
- Gates, R. A., Gauna, M., Morley, T. A., O'Donnell Jr, J. R., Smith, G. E., Watkins, T. R. & Zelanko, J. C. 2008. *Report of investigation: underground coal mine, fatal underground coal burst accidents, August 6 and 16, 2007, Crandall Canyon mine*, Genwal Resources, Inc. Huntington, Emery County, Utah, ID, (42-01715).

10. Gu, R., 2013 Distinct Element Model Analyses of Unstable Failures in Underground Coal Mines, [Ph.D. thesis]: Golden, Colorado School of Mines.
11. Rice, J. R. 1983. Constitutive relations for fault slip and earthquake instabilities. *Pure and applied geophysics*, 121(3), 443-475.